Hindawi
International Journal of Antennas and Propagation
Volume 2017, Article ID 7253623, 9 pages
https://doi.org/10.1155/2017/7253623

Research Article

Measured Performance Comparisons between Spatial Multiplexing and Beamforming Arrays in the 28 GHz Band

Dazhi Piao, Xingning Jia, Xiaochuan Ma, Qingxin Guo, and Zengrui Li

Department of Communication Engineering, Communication University of China, Beijing 100024, China

Correspondence should be addressed to Dazhi Piao; piaodazhi@hotmail.com

Received 31 October 2016; Revised 3 January 2017; Accepted 6 February 2017; Published 23 March 2017

Academic Editor: Rausley A. A. De Souza

A spatial multiplexing (SM) array and a beamforming (BF) array with similar antenna size working at 28 GHz are designed and fabricated. In the SM array, a 4 × 4 MIMO system is realized with each port composed of a four-element subarray. In the BF array, the whole 16 elements are used to formulate a high-gain array. The measured *S*-parameters are in agreement with the simulated results. For both arrays, the channel capacities are computed by the measured channel matrix and signal-to-noise ratio (SNR) in an office room. Results show that capacity of the SM system is larger than that of the BF system, although the gain of BF array is about 5 dB larger than that of the SM array. However, the capacity of the SM array depends heavily on SNR; specifically, for the 1 dBm transmit power, communication distance $R = 25$ cm, the ergodic capacity of the SM system is 2.76 times that of the BF system, and if $R = 250$ cm, the capacity gain is reduced to 1.45. Furthermore, compared with the BF array, the SM array has a more robust performance over antenna misalignment, because of the wider beamwidth.

1. Introduction

Millimeter wave (mmW) has been attracting increased attention in the 5th-generation (5G) wireless systems [1], because huge amount of raw bandwidth is available for wireless communication services. In addition, the small wavelengths of this band make the use of a large number of antenna elements at the base station as well as the user equipment to formulate a multiple-input multiple-output (MIMO) system possible. Although MIMO techniques have been widely employed in cellular and wireless local area network systems working at sub-6 GHz [2–4], the potential and realization of MIMO technique in mmW band were still not fully understood, considering the unique multipath propagation characteristics and the increased path loss over the lower frequency bands used in current 3G/4G wireless communication.

Spatial multiplexing (SM) and beamforming (BF) are the most commonly used two approaches to realize a MIMO system. In a SM system, the whole information stream is divided into multiple pieces [5], each of which is transmitted simultaneously and parallel on the same frequency band through different antenna ports. The multiplexing gain can be obtained by exploiting the spatial difference of the channel response in different transmit (Tx)-receive (Rx) element pair. On the other hand, in the mmW band, the propagation loss is higher compared to the lower frequencies; thus, the high-gain antenna arrays are expected to compensate for the increased path loss. In the systems with MIMO technique working at lower frequencies, such as LTE, digital BF with per-element weight adaptation to provide the best matching to the instantaneous channel state information can be realized. However, for mmW systems with large number of antenna elements, such a digital BF is infeasible in the near term, due to the cost of the large number of RF chains and mixed signal components [6, 7]. Thus, BF in this paper is considered to be realized at analog domain, where networks of phase shifter are used to formulate a directed beam patterns, focusing the array gain in the dominant propagation directions.

Some researches have been conducted on the performance of SM and BF in the mmW communications. The effect of BF on the improvement of some channel metrics of the indoor 60 GHz band system has been studied by measurements [8]; the performance of random beamforming has been analyzed for sparse mmW multiuser downlink channel based on a uniform random multipath channel model [9]. The feasibility of indoor mmW MIMO has been

investigated by ray-tracing based channel modeling [10, 11], by virtual antenna array based channel measurement [11, 12], and also by a 2 × 2 microstrip array in an underground mine environment [13]. A generalized spatial modulation MIMO scheme in indoor line-of-sight (LOS) mmW communication at 60 GHz is proposed and analyzed [14]. Furthermore, the suitability of SM and BF in the mmW band has also been studied by measurement-based statistical channel modeling [15, 16] in outdoor cellular environments and by the plane and spherical wave expressed channel modeling along with the virtual array based indoor experiments [17]. The performance of a hybrid transmission combining BF and SM in mmW communication is also analyzed based on a ray-tracing method in both LOS and multipath environment [18].

Given the Tx and Rx antenna aperture size and working frequency, the maximum number of antenna elements that could be supported is fixed. If more antenna ports are formulated for SM, the number of parallel subchannels will be increased but with a reduced subarray gain; on the contrary, if more antenna elements are used for BF, the array gain will be increased but the number of multiplexing channels will be reduced. Thus, a tradeoff between SM and BF should be made in the massive antenna mmW wireless systems, and which one has a better capacity performance depends on the radiation characteristics of the antennas, the multipath distribution, and the path loss of the particular environment. To make the tradeoff between SM and BF at mmW frequencies, channel measurements with respect to realistic antenna array configurations and propagation environments are required, yet, to date, there has been little such work about the performance comparisons between SM and BF in the mmW wireless communications.

In this paper, we provide the measurement-based channel capacity comparison between SM and BF under realistic antenna arrays, with the same Tx power, the same array position, and the same propagation condition. In particular, given the size of antenna aperture, there are totally 16 linearly polarized antenna elements working at 28 GHz, realized by a kind of L-probe microstrip antenna [19]. In the SM system, it is divided into 4 subarrays, and each consists of 4 elements, which corresponds to a 4 × 4 MIMO system. In the BF system, the antenna array is constructed by the whole 16 elements, which corresponds to a SISO system but with a larger array gain than that of the SM system. The results in this paper provide guidance for the design and application of SM and BF subarrays in the massive MIMO systems in the short-range indoor mmW scenarios, with the realistic array geometry, propagation characteristic, and SNR.

2. SM and BF Arrays Design

A coplanar waveguide (CPW) feed microstrip antenna array realized by a single layer printed circuit board technique is designed, because of the low material cost, planer structure, and ease of fabrication. Firstly, a subarray composed of 4 elements is constructed, as shown in Figure 1. Here, the defected ground technique is adopted to get a better impedance matching.

Table 1: Dimensions of the antenna element.

Parameter	Value (mm)
W	4.4
L	3.3
F_p	1.7
F_w	1.2
F_1	2.5
g_2	0.15
T	0.508
C_1	0.56
H_1	9
C_2	1.5
W_2	1.2
W_3	0.15
S_1	1.65
S_2	2
W_1	1.2
g	0.15
V_1	8.4

The dimensions of this 4-element array are shown in Table 1, and the detailed meaning of those parameters can be found in [19]. Based on this 4-element subarray, the SM array and BF array are constructed. A photograph of the fabricated SM and BF antenna is shown in Figure 2. The Rogers Duroid 5880 substrate ($\varepsilon_r = 2.2$ and $\tan\delta = 0.0009$) is selected with a thickness of 0.508 mm.

The antennas are modeled and simulated using the Ansoft's HFSS full-wave simulator. The reflection and transmission coefficients are given in Figures 3 and 4, respectively. Those figures show that the measured and simulated S-parameters of the SM and BF array basically agree with each other. The measured return losses of the 4 ports in the SM antenna and that of the BF antenna are all below the −10 dB between 27.2 GHz and 29 GHz. Moreover, all the measured isolations among the 4 ports of the SM antenna are better than −25 dB.

In Figure 5 the array gain of the BF antenna and the SM antenna in different ports are illustrated, which shows that good agreements between the simulated and the measured results exist. The gain of the BF array is about 5 dB higher than that of the SM array, which has small difference in different port due to tiny deviations in the dimensions and the variations in the feeding lines of the fabricated antennas. In Figure 6, the measured yz plane radiation characteristics of the two arrays at 28 GHz are illustrated. It is shown that the SM antenna has a wider radiation pattern than that of the BF antenna; specifically, the 3 dB beamwidth of the SM array is 37.9° and that of the BF array is only 12.3°.

3. Measurement Experiment

3.1. Experiment Setup. The measurement scenario is an office room located on the 9th floor of the main building of the Communication University of China, with the dimensions

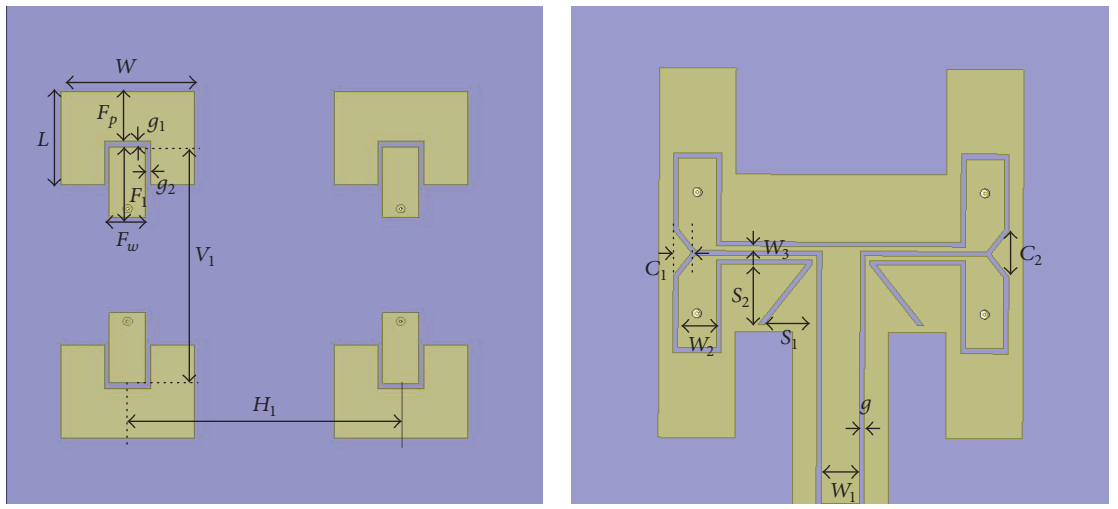

(a) (b)

FIGURE 1: Geometry of the subarray composed of 4 elements. (a) Top view. (b) Bottom view.

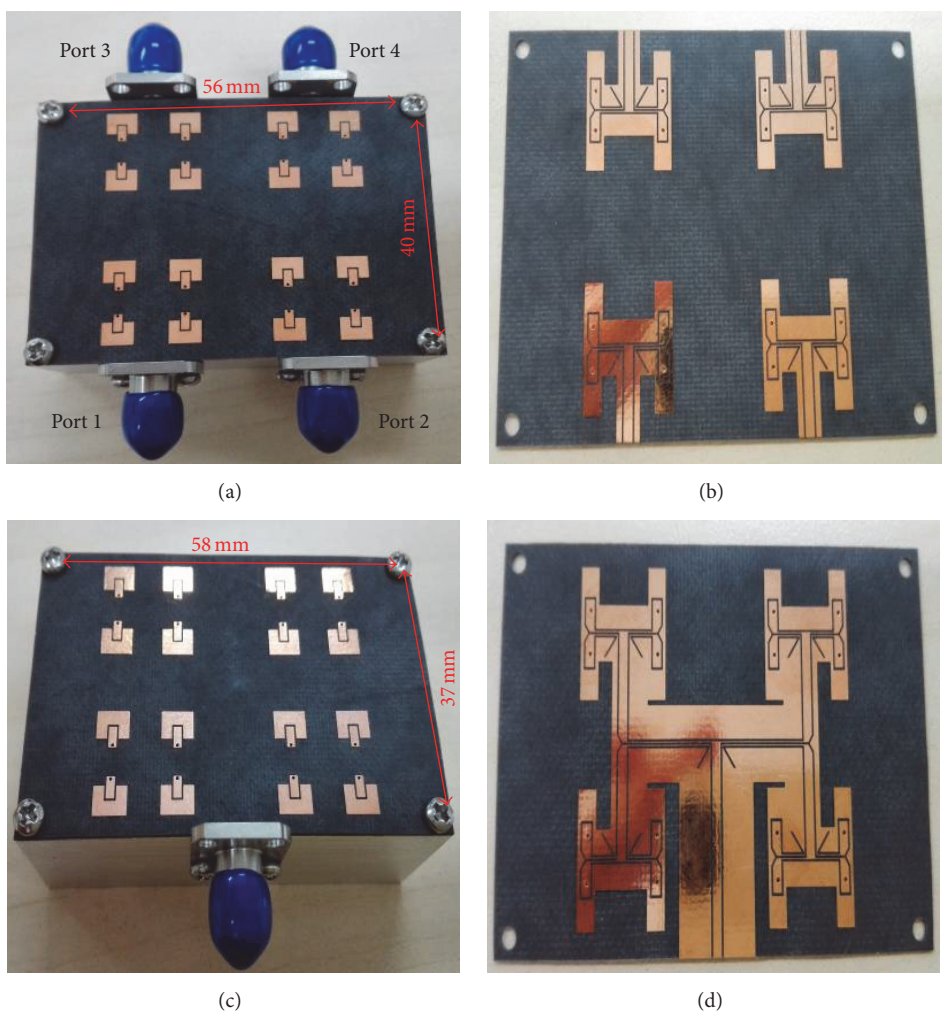

(a) (b)

(c) (d)

FIGURE 2: The fabricated SM and BF antenna. (a) Perspective view and (b) bottom view of the 4-port SM array. (c) Perspective view and (d) bottom view of the one-port BF array.

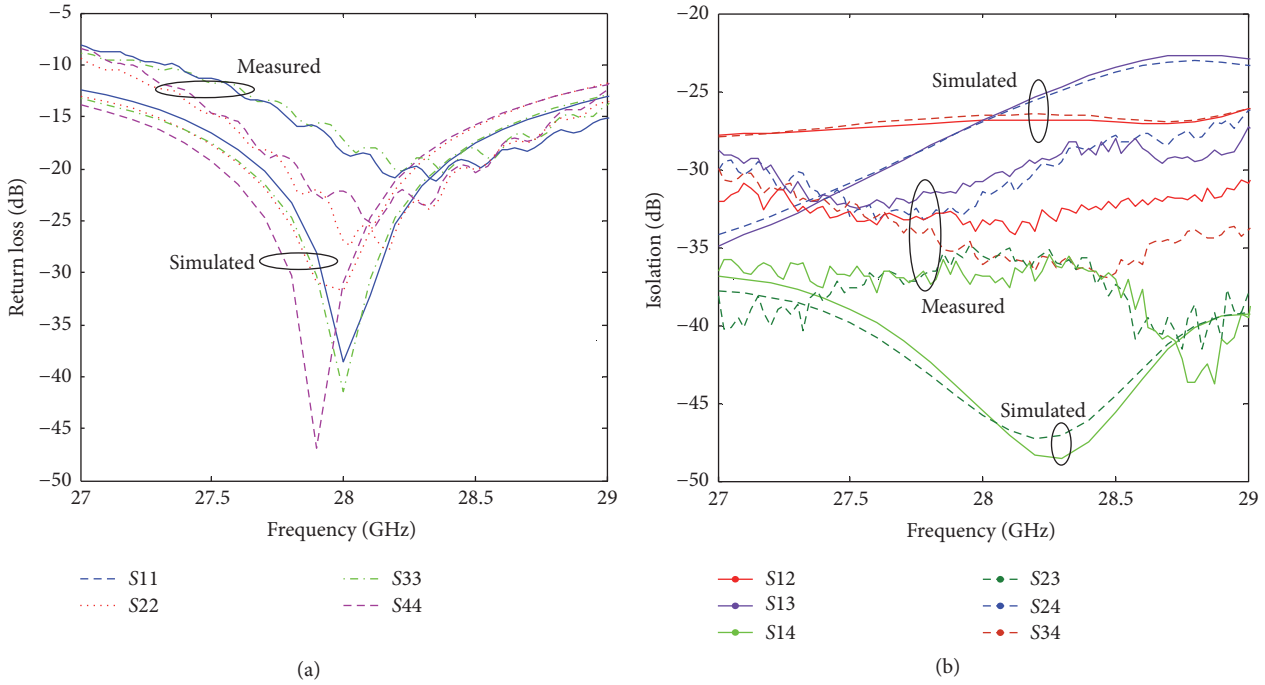

Figure 3: Simulated and measured S-parameters of the SM array. (a) Return loss. (b) Isolation.

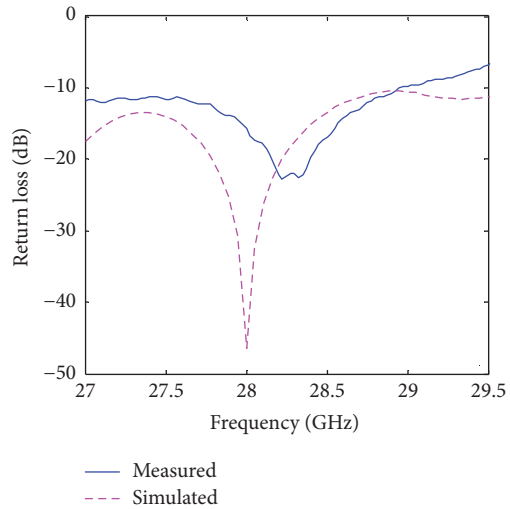

Figure 4: Simulated and measured S-parameters of the BF array.

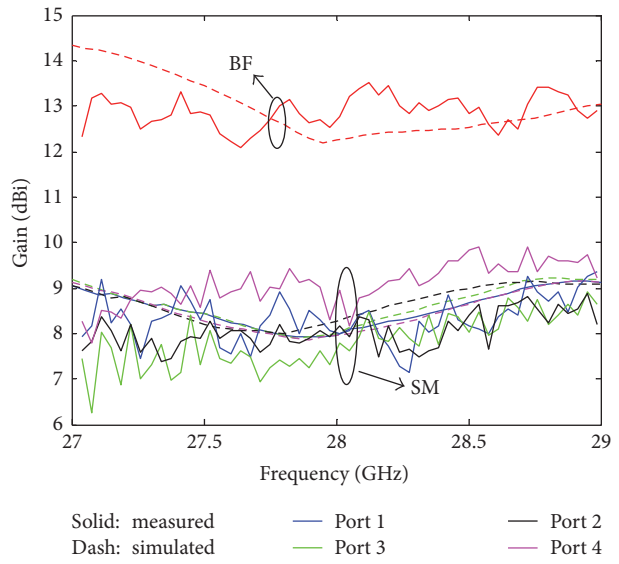

Figure 5: Simulated and measured gains of the SM and BF antenna array.

of 2.6 m × 5.6 m× 3.2 m ($W \times L \times H$). As shown in Figure 7, along the walls, there are some tables, computers, and experiment devices. The office room has one wooden door and several glass windows. The frame works of the building are reinforced concrete, and the walls and floors consist mainly of brick and plaster. During the experiment, the Tx antenna is fixed, and the Rx antenna is located in different positions. The scattering parameters are measured by a vector network analyzer (VNA) Agilent N5234A. Firstly, the fabricated SM array is employed at both the Tx and Rx ends, and each Tx port and Rx port are connected to the input and output ports of the VNA. The system is thoroughly calibrated to eliminate frequency-dependent attenuation and phase distortion. Between the Tx and Rx array, there are no obstacles to insure LOS propagation existed for all positions.

The real-time S-parameters from VNA are saved by a computer automatically. The 4 × 4 channel matrix $\mathbf{H}$ was determined by measuring the transfer parameters between each pair of the Tx and Rx antenna ports, with the remaining ports terminated by matched loads. For each position of the

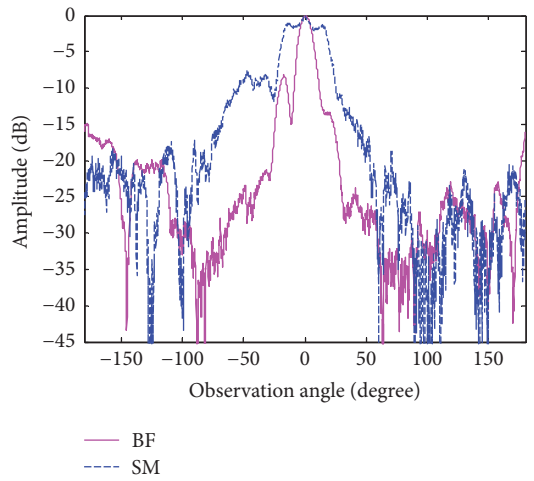

Figure 6: Measured radiation patterns of the SM and BF antenna array.

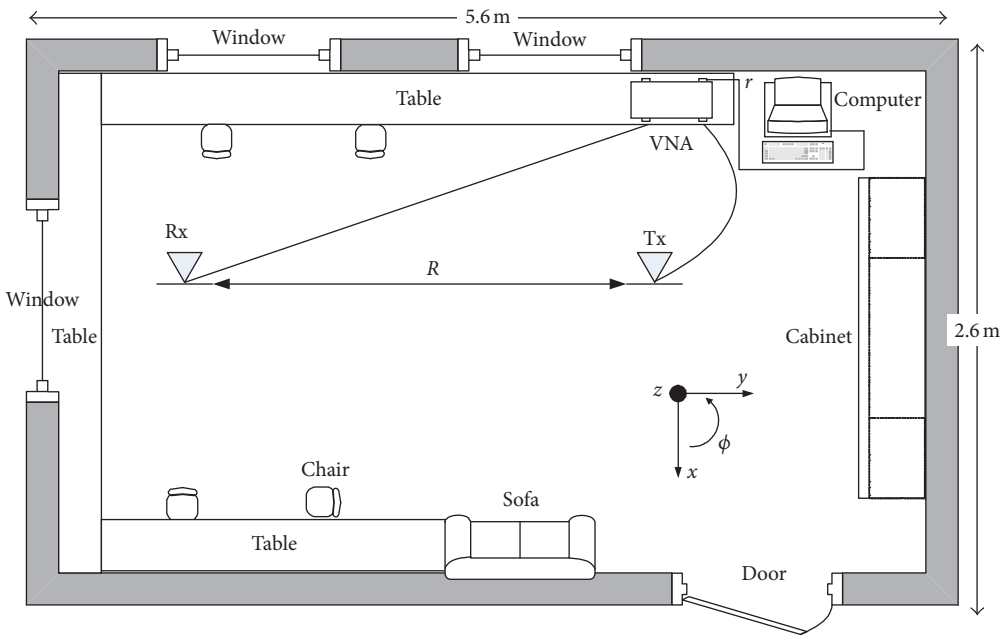

Figure 7: Measurement location and the schematic of the room.

Rx antenna, the data is recorded over 40 seconds with the sampling interval of 1 second. Over the working bandwidth of 27.2–29 GHz, with step sizes of 12.5 MHz, there are totally 145 frequency points. Thus, for each Tx and Rx antenna pair, the total number of measured channels is $145 \times 40 = 5800$. Then the measurement procedure is repeated for both the Tx and Rx ends are equipped with the BF array, with exactly the same Tx power and the antenna position. The personnel movement is kept to a minimum to ensure the statistical stationarity of the propagation.

3.2. Results. The performance of a MIMO system is generally evaluated by the channel capacity. If the channel state information is not available at the Tx end, the equal power allocation at each port is generally used, and the corresponding channel capacity can be computed by [5]

$$C = \log_2 \det\left(\mathbf{I} + \left(\frac{\mathrm{SNR}}{n_T}\right)\mathbf{H}\mathbf{H}^{\dagger}\right), \quad (1)$$

where $\mathbf{I}$ is the identity matrix, SNR is the signal-to-noise ratio, n_T is the number of transmit antennas, and $\mathbf{H}^{\dagger}$ means the transpose conjugate of $\mathbf{H}$. In most of the pervious works, the channel matrix is normalized, and the capacity is computed with the assumed SNR values. By this method, only the effect of richness of the multipath on MIMO performance can be evaluated.

In this paper, we also used the normalized channel matrix; however, the real values of average received SNR for different antenna positions are measured and used in the capacity calculation, through which the effect of actual received power on the system property can be illustrated.

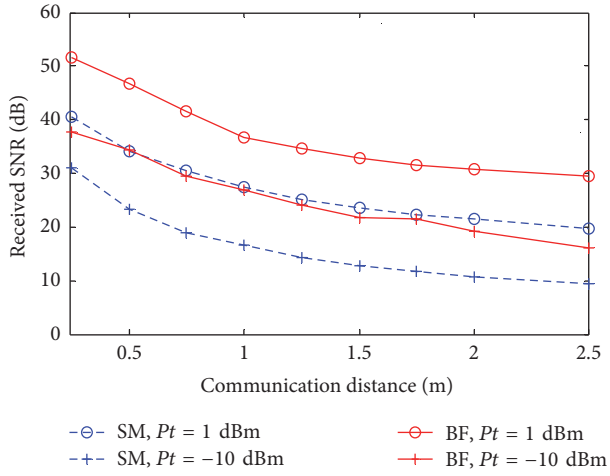

FIGURE 8: Relationship between the averaged received SNR and R.

Firstly, the variations of SNR and channel capacity with communication distance R are investigated. During the measurement, both the Tx and Rx antennas are vertically polarized and with the equal height to the floor $h_t = h_r = 118$ cm. The maximum radiation directions of Tx and Rx antennas are aligned to obtain the best LOS signal level. The position of the Tx antenna is fix, and the Rx antenna is moved away gradually from the Tx antenna, with R increased from 25 cm to 250 cm. To get the value of SNR, we measured the received power of the background noise and that of the transmitted signal, individually, and then calculated the ratio between them. The relationship between the received SNR and communication distance is shown in Figure 8, for each position, the SNR value is an averaged result over all the 5800 samples, and the result of SM array is the averaged value over 4 ports. As can be seen from Figure 8, for short range with R smaller than 1 m, the decreasing slope of SNR curve is obviously larger than that of the larger range. Furthermore, the SNR obtained by the BF array is about 7–10 dB larger than that of the SM array, which is basically consistent with the measured array gains.

It is well known that, besides SNR, the MIMO capacity also depends heavily on correlation properties of the channel matrix, which is decided by the complex interaction between antenna radiation characteristic and the surrounding environment. A MIMO system can only perform well if the channel elements are statistically independent [20]. In Figure 9, the Rx correlation coefficients (CCs) with respect to Tx port 1 of the SM array are described, and the results corresponding to other Tx ports are similar. Figure 9 tells us that, for $R = 25$ cm, the CCs are comparatively high due to the dominating contribution of the LOS signal, and, for larger communication distance, the CCs get smaller, because the contributions of multipath components get larger. However, even the CCs in Figure 9(a) are not very high, which have almost no negative impact on the performance of the MIMO system.

In Figure 10, the cumulative distribution functions (CDFs) of the channel capacity corresponding to the 4 × 4 SM MIMO system and that of the BF SISO system are compared, with the increasing of communication distance. For each curve, it is the statistical result based on 5800 samples. The corresponding ergodic capacity has also been calculated based on these CDF results. From Figure 10(a), for $P_t = 1$ dBm, if $R = 25$ cm, the ergodic capacity of the SM system is 2.76 times that of the BF system; however, if $R = 250$ cm, the capacity gain is reduced to only 1.45. From Figure 10(b), for $P_t = -10$ dBm, the corresponding ergodic capacity gain drops slightly, 2.43 and 1.37, respectively. Results in Figure 10 indicate that, in the SM array MIMO system, large capacity gain can only be obtained with a sufficiently high SNR.

Figure 10 gives the results of the Tx and Rx antennas best aligned to get the largest SNR; however, in the actual communications, the antennas cannot be always adjusted to the best direction. Thus, the performances of these arrays with angle deviations from the best one are also investigated in Figure 11, in the azimuth (φ) and elevation (θ) angle plane, individually. In the measurement of Figure 11(a), $P_t = 1$ dBm, h_t and h_r are also set to 118 cm, and R is kept as a constant of 1 m. The position of Rx is changed, to make the azimuth deviation angle with respect to the maximum radiation direction gradually increase from 0° to 25°. As to the test in Figure 11(b), the position of Tx is also fixed with $h_t = 118$ cm, h_r is increased gradually to get an incremental elevation angle deviation, and the horizontal distance between the Tx and Rx is kept also as 1 m.

Figure 11 shows that, with the increasing of angle deviation from both the horizontal and vertical planes, the channel capacity obviously declines; however, it behaves differently for different arrays and shows a strong dependence on the antenna radiation pattern. In particular, the SM array has a more robust performance over the angle deviation in the horizontal plane; as calculated by the data in Figure 11(a), if $\varphi = 10°$, the ergodic capacity drop is only 1.85% for the SM array, whereas the value for the BF array is 27.03%. In the vertical plane, performances of both arrays degrade quickly with the increase of θ, and if $\theta = 10°$, as calculated by the data in Figure 11(b), the drop in ergodic capacity will reach 30.53% and 26.56% for the SM array and BF array, respectively. The results in Figure 11 could be explained that, in the horizontal plane, the SM array has a wider radiation pattern than that of the BF array, but, in the vertical plane, there are no obvious differences.

4. Conclusion

A BF SISO array and a SM MIMO array with 4 ports working at 28 GHz are designed and fabricated, with totally 16 antenna elements. To make a comparison and tradeoff between the channel capacities of those arrays, their channel responses are measured and compared in an indoor office room. The dependence of the channel capacity of both arrays on communication distance is computed with the actual received SNR. Furthermore, the effects of antenna array misalignment on the degradation of the channel capacity are also investigated, both in the azimuthal and in the elevation angle plane. It is found that although the BF array can get a

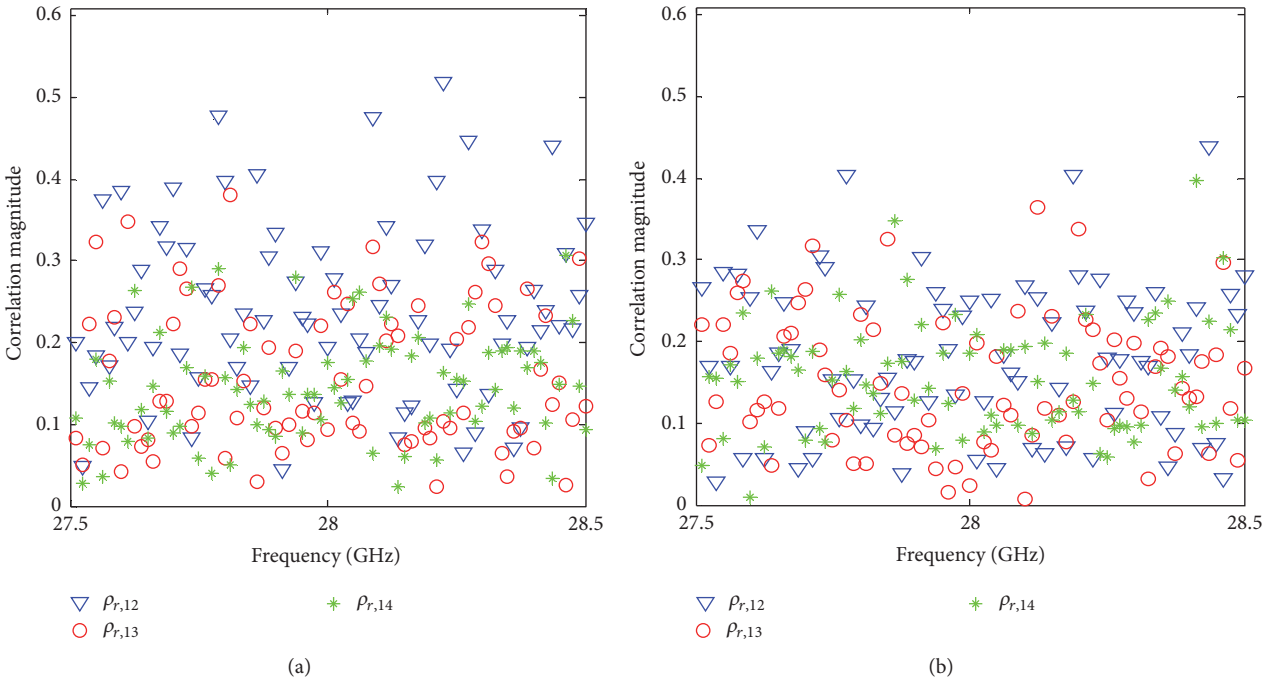

FIGURE 9: Dependence of the receive correlation coefficients on frequency. (a) $R = 25$ cm. (b) $R = 125$ cm.

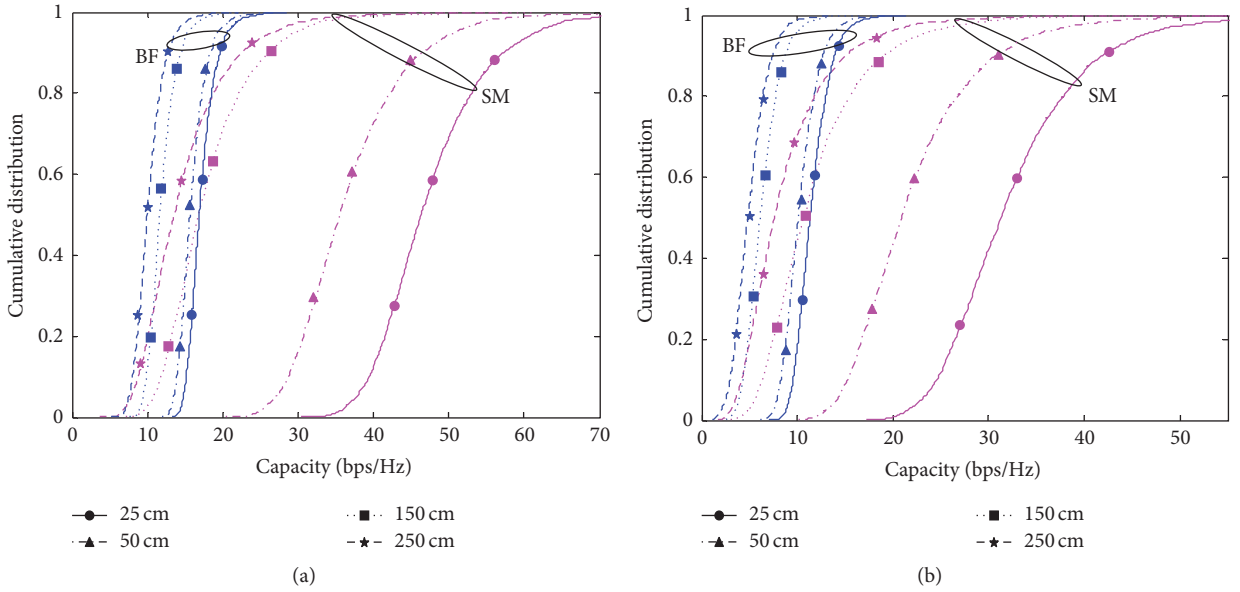

FIGURE 10: Dependence of capacity on R. (a) $P_t = 1$ dBm. (b) $P_t = -10$ dBm.

concentrated and directed beam pattern to get an increased SNR, the SM array can still get a larger channel capacity, thanks to the spatial multiplexing gain obtained in the MIMO channel, and thus the incoming data stream can be divided into several parallel substreams transmitted simultaneously. High spatial multiplexing gain obtained by the SM array in the indoor office room in 28 GHz can be explained that, for shorter distance, such as $R = 0.25$ m, enough difference of the channel responses in space can be obtained since the subarray spacing is about 2.1 λ, and, for longer distance, the channel provides enough multipath angular spread which is beneficial for the channel decorrelation.

Furthermore, the SM array has a more robust performance over the antenna misalignment because of the wider radiation pattern. However, the large channel capacity gain of the SM array can only be obtained with a sufficiently high SNR. Here, we only considered a mmW array with totally 16 antenna elements, for the arrays with larger size and more elements, there will be more realizations of the MIMO array, and which one has a better and more robust performance

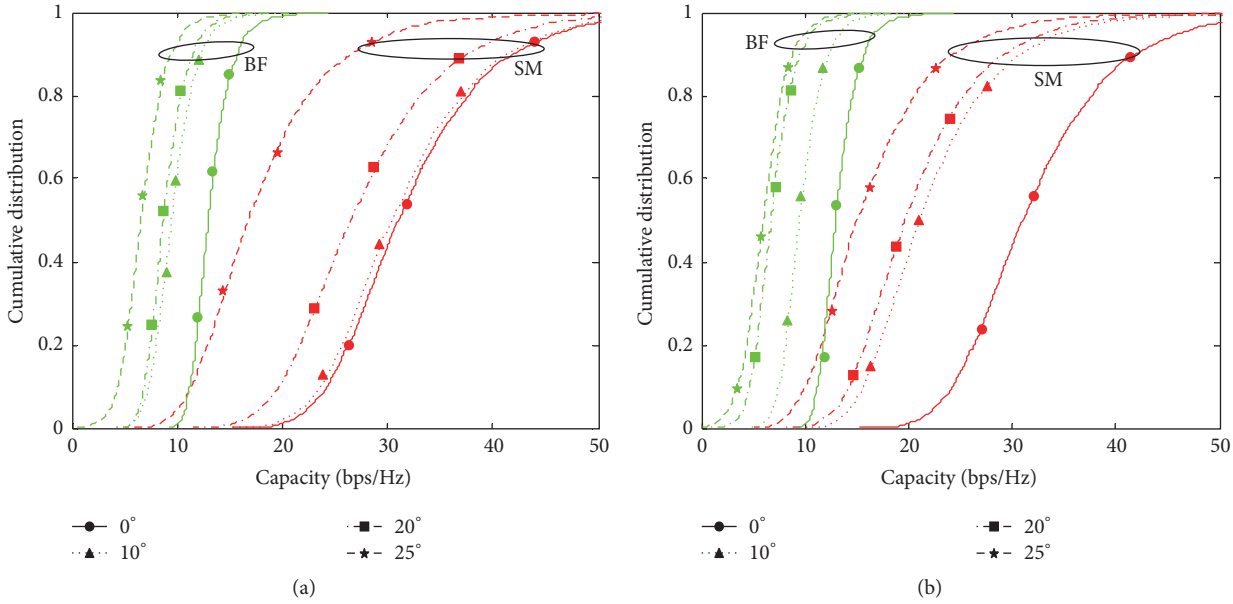

Figure 11: Dependence of capacity on the deviation angle. (a) Azimuth plane. (b) Elevation plane.

will be investigated in the future by measurement as well as theoretical modeling.

Conflicts of Interest

The authors declare that there are no conflicts of interest regarding the publication of this paper.

Acknowledgments

This work was supported by the National Natural Science Foundations of China (Grant no. 61201235) and the Young Talents Program of Beijing Universities (no. YETP0595).

References

[1] F. Boccardi, R. Heath Jr., A. Lozano, T. L. Marzetta, and P. Popovski, "Five disruptive technology directions for 5G," *IEEE Communications Magazine*, vol. 52, no. 2, pp. 74–80, 2014.

[2] H. Sampath, S. Talwar, J. Tellado, V. Erceg, and A. Paulraj, "A fourth-generation MIMO-OFDM broadband wireless system: design, performance, and field trial results," *IEEE Communications Magazine*, vol. 40, no. 9, pp. 143–149, 2002.

[3] Q. Li, G. Li, W. Lee et al., "MIMO techniques in WiMAX and LTE: a feature overview," *IEEE Communications Magazine*, vol. 48, no. 5, pp. 86–92, 2010.

[4] J. Kim and I. Lee, "802.11 WLAN: history and new enabling MIMO techniques for next generation standards," *IEEE Communications Magazine*, vol. 53, no. 3, pp. 134–140, 2015.

[5] G. J. Foschini and M. J. Gans, "On limits of wireless communications in a fading environment when using multiple antennas," *Wireless Personal Communications*, vol. 6, no. 3, pp. 311–335, 1998.

[6] A. Alkhateeb, J. Mo, N. González-Prelcic, and R. W. Heath Jr., "MIMO precoding and combining solutions for millimeter-wave systems," *IEEE Communications Magazine*, vol. 52, no. 12, pp. 122–131, 2014.

[7] J. Singh and S. Ramakrishna, "On the feasibility of codebook-based beamforming in millimeter wave systems with multiple antenna arrays," *IEEE Transactions on Wireless Communications*, vol. 14, no. 5, pp. 2670–2683, 2015.

[8] S. Wyne, K. Haneda, S. Ranvier, F. Tufvesson, and A. F. Molisch, "Beamforming effects on measured mm-wave channel characteristics," *IEEE Transactions on Wireless Communications*, vol. 10, no. 11, pp. 3553–3559, 2011.

[9] G. Lee, Y. Sung, and M. Kountouris, "On the performance of random beamforming in sparse millimeter wave channels," *IEEE Journal on Selected Topics in Signal Processing*, vol. 10, no. 3, pp. 560–575, 2016.

[10] E. Torkildson, U. Madhow, and M. Rodwell, "Indoor millimeter wave MIMO: feasibility and performance," *IEEE Transactions on Wireless Communications*, vol. 10, no. 12, pp. 4150–4160, 2011.

[11] M.-T. Martinez-Ingles, D. P. Gaillot, J. Pascual-Garcia, J.-M. Molina-Garcia-Pardo, M. Lienard, and J.-V. Rodríguez, "Deterministic and experimental indoor mmW channel modeling," *IEEE Antennas and Wireless Propagation Letters*, vol. 13, pp. 1047–1050, 2014.

[12] S. Ranvier, C. Icheln, and P. Vainikainen, "Measurement-based mutual information analysis of MIMO antenna selection in the 60-GHz band," *IEEE Antennas and Wireless Propagation Letters*, vol. 8, pp. 686–689, 2009.

[13] I. Ben Mabrouk, J. Hautcoeur, L. Talbi, M. Nedil, and K. Hettak, "Feasibility of a millimeter-wave MIMO System for short-range wireless communications in an underground gold mine," *IEEE Transactions on Antennas and Propagation*, vol. 61, no. 8, pp. 4296–4305, 2013.

[14] P. Liu, M. Di Renzo, and A. Springer, "Line-of-sight spatial modulation for indoor mmWave communication at 60 GHz," *IEEE Transactions on Wireless Communications*, vol. 15, no. 11, pp. 7373–7389, 2016.

[15] M. R. Akdeniz, Y. Liu, M. K. Samimi et al., "Millimeter wave channel modeling and cellular capacity evaluation," *IEEE Journal on Selected Areas in Communications*, vol. 32, no. 6, pp. 1164–1179, 2014.

[16] S. Sun, T. S. Rappaport, R. W. Heath, A. Nix, and S. Rangan, "MIMO for millimeter-wave wireless communications: beamforming, spatial multiplexing, or both?" *IEEE Communications Magazine*, vol. 52, no. 12, pp. 110–121, 2014.

[17] K. Haneda, C. Gustafson, and S. Wyne, "60 GHz spatial radio transmission: multiplexing or beamforming?" *IEEE Transactions on Antennas and Propagation*, vol. 61, no. 11, pp. 5735–5743, 2013.

[18] S. J. Lee and W. Y. Lee, "Capacity of multiple beamformed spatial stream transmission in millimetre-wave communication channels," *IET Communications*, vol. 7, no. 12, pp. 1263–1268, 2013.

[19] M. Li and K.-M. Luk, "Low-cost wideband microstrip antenna array for 60-GHz applications," *IEEE Transactions on Antennas and Propagation*, vol. 62, no. 6, pp. 3012–3018, 2014.

[20] D. Piao, L. Yang, Q. Guo, Y. Mao, and Z. Li, "Measurement-based performance comparison of colocated tripolarized loop and dipole antennas," *IEEE Transactions on Antennas and Propagation*, vol. 63, no. 8, pp. 3371–3379, 2015.